Global Change Biology
celebrating 20 years
Global Change Biology (2014), doi: 10.1111/gcb.12463

Rainfall and temperatures changes have confounding impacts on *Phytophthora cinnamomi* occurrence risk in the southwestern USA under climate change scenarios

SALLY E. THOMPSON[1], SIMON LEVIN[2] and IGNACIO RODRIGUEZ-ITURBE[3]
[1]*Department of Civil and Environmental Engineering, University of California, Berkeley, CA 94710, USA,* [2]*Department of Ecology and Evolutionary Biology, Princeton University, Princeton NJ 08544, USA,* [3]*Department of Civil and Environmental Engineering, Princeton University, Princeton, NJ 08544, USA*

Abstract

Global change will simultaneously impact many aspects of climate, with the potential to exacerbate the risks posed by plant pathogens to agriculture and the natural environment; yet, most studies that explore climate impacts on plant pathogen ranges consider individual climatic factors separately. In this study, we adopt a stochastic modeling approach to address multiple pathways by which climate can constrain the range of the generalist plant pathogen *Phytophthora cinnamomi* (Pc): through changing winter soil temperatures affecting pathogen survival; spring soil temperatures and thus pathogen metabolic rates; and changing spring soil moisture conditions and thus pathogen growth rates through host root systems. We apply this model to the southwestern USA for contemporary and plausible future climate scenarios and evaluate the changes in the potential range of Pc. The results indicate that the plausible range of this pathogen in the southwestern USA extends over approximately 200 000 km^2 under contemporary conditions. While warming temperatures as projected by the IPCC A2 and B1 emissions scenarios greatly expand the range over which the pathogen can survive winter, projected reductions in spring rainfall reduce its feasible habitat, leading to spatially complex patterns of changing risk. The study demonstrates that temperature and rainfall changes associated with possible climate futures in the southwestern USA have confounding impacts on the range of Pc, suggesting that projections of future pathogen dynamics and ranges should account for multiple pathways of climate–pathogen interaction.

Keywords: California, climate change, edaphic, multiple stressors, *Phytophthora cinnamomi*, plant pathogen, rainfall, stochastic modeling

Received 18 June 2013 and accepted 22 October 2013

Introduction

The potential for warmer temperatures to expand pathogen ranges and alter epidemiology is an important consequence of global climate change for human populations and the environment (Coakley *et al.*, 1999; Chakraborty *et al.*, 2000; Bergot *et al.*, 2004; Boland *et al.*, 2004; Garrett *et al.*, 2006; Ibanez *et al.*, 2006; Pautasso *et al.*, 2010). Plant pathogens influence large-scale forest mortality events, so understanding their future range and impacts will assist conservation planning (Allen *et al.*, 2010; Jactel *et al.*, 2012). Plant pathogens also impact agricultural production, meaning their response to climate change threatens global and regional food security (Chakraborty, 2005; Sutherst *et al.*, 2011). Pathogens are sensitive to multiple climatic and environmental factors, as reflected in the 'disease triangle' (Agrios, 2005), a conceptual model that states that disease is the outcome of the presence of a virulent pathogen, a susceptible host, and suitable environmental conditions. Theoretical and empirical studies addressing climate change impacts on plant disease tend to focus on individual environmental factors such as temperature (Chakraborty, 2005; Garrett *et al.*, 2006; Thompson *et al.*, 2010), elevated atmospheric carbon dioxide concentrations (Pangga *et al.*, 2004; Lake & Wade, 2009; Melloy *et al.*, 2010) and water availability (Desprez-Loustau *et al.*, 2006; Thompson *et al.*, 2013), despite the likelihood that climate change will alter temperature, precipitation, potential evaporation, and ecological regimes simultaneously. Retrospective analyses show that multiple environmental drivers and their interactions influence expansion of disease ranges (Fabre *et al.*, 2011; Pangga *et al.*, 2011). Understanding these interactions remains an area of outstanding research need (Chakraborty, 2005; Pautasso *et al.*, 2012).

Climatic and edaphic factors could limit *Phytophthora cinnamomi* (Pc) range in several ways. First, Pc is sensitive to cold temperatures (approaching freezing). Exposure to sufficiently cold temperatures for sufficiently long durations during winter will kill Pc (Marçais *et al.*, 1996). Temperatures warm enough to permit survival of Pc may still be cold enough to suppress its ability to

Correspondence: Sally Thompson, tel. +1 510 642 1980, fax +1 510 643 5264, e-mail: sally.thompson@berkeley.edu

grow, reproduce, and cause disease to hosts (Zentmyer *et al.*, 1976; Shearer *et al.*, 1987). Previous modeling studies considering temperature effects on Pc range in Europe suggest the potential for considerable expansion in warming climates (Brasier & Scott, 1994; Bergot *et al.*, 2004). However, Pc growth rates also display a threshold-like response to soil moisture in laboratory conditions. Dry soils also inhibit reproduction, survival, dispersal, and development of symptoms in host plants (Hwang & Ko, 1978; MacDonald & Duniway, 1978; Nesbitt *et al.*, 1978; Malajczuk & Theodorou, 1979; Benjamin & Newhook, 1981; Tippett *et al.*, 1987, 1989). Soil moisture conditions experienced by the pathogen themselves arise from interactions among the precipitation regime, soil depth, drainage, and atmospheric evaporative demand, and thus reflect the interplay of edaphic and climatic conditions. Finally, Pc disease is also often suppressed in rich soils where organic matter content exceeds ≈5% (Broadbent & Baker, 1974; Nesbitt *et al.*, 1979), probably because of predation by other soil organisms in the diverse microfaunal communities sustained in these soils (Weste & Marks, 1987).

Projections of potential future risk therefore require techniques to assess the impact of multiple environmental changes and their interactions on pathogen range and epidemiology. Here, we apply a mechanistic modeling approach to explore how climate change could impact pathogen range and activity. We explore how simultaneous changes in temperature, precipitation, snow-pack extent, and evaporative demand might impact the range of a well-characterized pathogen under different climate scenarios. To do this we couple two existing models that describe controls on the range of the generalist root pathogen Pc in the state of California and surrounding regions in the states of Oregon, Nevada, and Arizona in the southwest USA. Pc occurs in this region (Tidwell *et al.*, 1984; Swiecki *et al.*, 2003; Garbelotto *et al.*, 2006; Chavarriaga *et al.*, 2007; Pagliaccia *et al.*, 2011, 2013) but its range is poorly delineated. In other warm climates such as southern Australia and Hawaii, Pc has had a devastating effect on timber production, natural forests and agriculture (Newhook & Podger, 1972; Hwang & Ko, 1978; Weste & Marks, 1987; Balci & Halmschlager, 2003; Harham, 2005; Judelson & Blanco, 2005; Benson *et al.*, 2006; Jönsson, 2006). Modeling the climatic and edaphic limits on its potential range in the US southwest will help determine the risks posed by this pathogen, particularly since there is not as yet a detailed understanding of the susceptibility of native species to Pc infection.

Our modeling study aims to address two research questions:

1. How do climate and edaphic factors limit the potential range of Pc in the southwestern USA under climatic conditions representative of the late 20th century (baseline conditions)? and
2. How do the different modes of Pc response to temperature and soil moisture change this projected range under plausible future climate scenarios?

Recognizing that observations of Pc in the region provide an incomplete delineation of the full potential Pc range, we nonetheless compare the location of known sites of Pc infection in California to the model predictions, as the most feasible check on the consistency of the model with observation.

Materials and methods

To address the research questions, we link two existing models that describe: (i) Pc winter survival probabilities and (ii) Pc disease severity during the spring growing season (when Pc typically expands through the root system of host species in Mediterranean climates such as those in the southwestern USA; Weste & Marks, 1987). We first model winter soil temperatures. Second, we use the modeled soil temperatures to estimate Pc survival with an existing, validated survival model (Marçais *et al.*, 1996). Next, we expand a probabilistic soil moisture model to account for snowpack contributions. We use the projected soil moisture fluctuations to drive a stochastic pathogen risk model, previously employed to describe disease range, relative risk on different soil types, and response to different irrigation regimes at sites in Western Australia and Oregon (Thompson *et al.*, 2013). The output of this model is a metric of the likelihood of disease expansion throughout a hosts' root system, lying between 0 (no Pc in the root system) and 1 (complete colonization of the root system). Fourth, we identify regions with high soil organic content from the national State Soil Geographic Database (STATSGO) and Soil Survey Geographic Database (SSURGO) data sets and exclude these regions from the potential Pc range (Scharwz & Alexander, 1995). Finally, we compute a relative Pc risk as the product of the risk of winter survival, absence of suppressive (organic) soil conditions, and moisture-controlled host colonization. We apply this modeling framework to baseline (approximately year 2000) and future (approximately year 2050) climate scenarios across the southwest USA. We repeat the analyses using high resolution downscaled climate and soil data for the San Francisco Bay Area (Flint & Flint, 2012), allowing us to explore the effects of microtopography, orography, and fine-grained changes in soil properties, typical of the California coastline, on the spatial patterns of Pc disease risk and its projected climate sensitivity.

Data sources

We use three different climate datasets: (i) monthly regional historical climate observations interpolated to a 140-km^2 grid for the 1950–2000 period (Maurer *et al.*, 2002); (ii) bias-corrected and spatially downscaled National Center for Atmospheric Research Community Climate System Model 3.0

(Collins *et al*., 2006) monthly simulations run for the IPCC A2 (medium-high emissions) and B1 (low emissions) climate scenarios on the same 140 × 140 km grid (Cayan *et al*., 2009; van Vuuren *et al*., 2011); and (iii) 30-year average monthly projections from the Geophysical Fluid Dynamics Laboratory climate models for the same scenarios, downscaled to a high resolution (270 × 270 m) grid over the San Francisco Bay area (Flint & Flint, 2012) for the 1970–2000 and 2035–2065 periods. To obtain representative climate characteristics, we average the monthly regional data over 10 year intervals (1990–2000 and 2045–2055). The climate components obtained for each dataset are summarized in Table 1. We estimate average daily temperature for the Bay Area climate surfaces as a simple mean of monthly maximum and minimum temperature; and estimate the potential evaporation at the southwestern US scale using the Priestly–Taylor equation.

One of the limitations of this approach lies in the considerable uncertainty surrounding the use of downscaled climate datasets. Our goal in using these high resolution data sets was to: (i) develop a reasonable baseline drawn from interpolated observations and (ii) compare this against plausible climate futures to elucidate the range of potential Pc responses and how they could manifest themselves at regional scales. We do not interpret these future cases as predictions or forecasts, but illustrative scenarios to offer insight into process interactions.

Regional soil data, specifically percentage clay, organic matter content and soil depth data are derived from STATSGO (Scharwz & Alexander, 1995). Soil data for the Bay Area are obtained from the SSURGO datasets (Staff, 2012). Both data sets derive from soil maps with irregular mapping units ranging from <1 ha in size to >20 000 ha (e.g., for large, homogeneous areas such as the submerged portions of San Francisco Bay). The soil data were thus mapped to the climate grid scales used for both the Bay Area and the regional scale. We use tabulated hydraulic parameters (Clapp & Hornberger, 1978) to estimate the properties of the water retention curve for each soil type on the basis of the percentage clay content, classifying <10% clay soils as sands, 10–15% clay content as loamy sands, 15–20% clay contents as sandy loams, 20–40% clay content as loams and >40% clay contents as clays. Georeferenced locations where Pc has been isolated from natural or agricultural soils in California were obtained from the Phytophthora Database (www.phytophthoradb.org), Forest Phytophthoras of the World (www.foresphytophthoras.org), and recent literature sources (Jacobs *et al*., 1997; Elliott *et al*., 2010; Swiecki *et al*., 2011).

Table 1 Data obtained for the regional and local climate characterization under baseline and future scenarios (Collins *et al*., 2006; Cayan *et al*., 2009; van Vuuren *et al*., 2011; Flint & Flint, 2012)

Scale	Datasets	Years
Local	Temperature (monthly max and min)	1970–2000, 2035–2065
	Potential evaporation (monthly mean)	
	Precipitation (monthly mean)	
Regional	Temperature (monthly mean)	1990–2000, 2045–2055
	Net radiation (monthly mean)	
	Relative humidity (monthly mean)	
	Snow water equivalent (monthly mean)	
	Precipitation (monthly mean)	

Winter survival modeling. Marçais *et al*. (1996) showed that winter survival of Pc declines as the duration of exposure to sub-zero temperatures increases, according to the relationship:

$$I = 1 - \frac{1}{1 + 14.7 \times \exp(0.007 \sum T_{<0})} \quad (1)$$

where $\Sigma T_{<0}$ represents the sum of hourly temperatures below 0 °C. Model validation showed that survival projections of 50% or greater corresponded to increases in disease symptoms in 86% of monitored stems, and no reductions in disease. Conversely, lower survival projections lead to reductions in disease symptoms or healing of previous wounding (Marçais *et al*., 1996). We therefore take survival projections of 50% or greater as providing an indication of plausible disease range as constrained by winter temperatures. To determine Pc exposure to these temperatures requires: (i) modeling soil temperature fluctuations with depth and (ii) estimating the maximum depth at which Pc occurs.

Several models have been proposed to estimate soil temperature dynamics using typical spatial datasets (Zheng *et al*., 1993; Kang *et al*., 2000). We use a recent version of these models that accounts for shading of the soil surface by vegetation and insulation of the soil surface by snow (Kätterer & Andrön, 2008). This model predicts T (z,t) the temperature of the soil at depth z and time t, as:

$$T_t(z) = T_{t-1}(z) + (T_{\text{surf}} - T_{t-1}(z)) \times \exp\left(-z\left(\frac{\pi}{K_s p}\right)^{1/2}\right) \times \exp(-k_{lb}\text{LAI}_t). \quad (2)$$

where T_{surf} is the surface temperature, K_s is the thermal diffusivity of the soil, p is a characteristic timescale of thermal fluctuations (in this case equivalent to the number of hours in 1 year), k_{lb} is the absorption coefficient associated with soil shading, and LAI is the leaf area index of local vegetation.

We assume that during winter, the surface temperature is given by the measured air temperature, that is, $T_{\text{surf}} = T_{\text{air}}$, except where a snow-pack is present to insulate the soil from air temperature fluctuations. We treat a monthly snow-water equivalent (SWE) >5 mm as indicating a persistent snowpack. In these cases, we follow Kätterer & Andrön (2008) in taking $T_{\text{surf}} = 0.2T_{\text{air}}$. Unfortunately, validation data for snow-covered surfaces are not available in the study region. The 20% factor was, however, extensively validated by Kätterer & Andrön (2008) in Europe.

Soil thermal diffusivity k_{sp} is computed with the methods of Peters-Lidard *et al*. (1998) (details in Appendix) using the mean soil moisture values computed in Section Pc - soil moisture model to give the percentage saturation of the winter soils. We calibrate the absorption coefficient k_{lb} for the soil

temperature model using data from 16 California Irrigation Management Information System (CIMIS) stations (http://wwwcimis.water.ca.gov/cimis/) spanning northern to southern California and representing coastal and interior sites. These stations report temperature data at 15 cm depth, over a 12-year timeframe (2000–2012). Assuming a reference LAI of 3 (Kätterer & Andrön, 2008), k_{lb} is calibrated by minimizing the mean absolute error in winter temperatures for all 16 stations (see Table 3), obtaining $k_{lb} = 0.96$.

Finally, we assume that during winter Pc organisms would preferentially migrate to deep soils that provide a thermal buffer against air temperature fluctuations. Although Pc is typically located in shallow soils with high plant root densities (Weste & Law, 1973), it has also been found at depths of up to 75 cm below the surface, when these soil conditions were more suitable for its growth, reproduction and survival (e.g., Shea *et al.*, 1983). We therefore compute the winter soil temperature profiles at the either the maximum soil depth or 75 cm depth, whichever is smaller, and insert these values into Eqn (2) to estimate Pc survival risk.

Pc - soil moisture model. Thompson *et al.* (2013) developed a stochastic model to relate Pc establishment risk to soil moisture dynamics (the mathematical details of this model are presented in expanded form in the Appendix). The stochastic soil moisture model of Laio *et al.* (2001) and its crossing properties as identified by Porporato *et al.* (2001) were used to estimate the frequency with which soil moisture conditions (represented by s, the relative moisture content, equivalent to the volumetric water content normalized by the soil porosity) fluctuate around a 'critical' matric potential (or equivalently a critical soil moisture, s_c). If the critical potential Ψ_c is set to the value at which dry soils inhibit Pc growth (approximately −3000 kPa in sterile laboratory media; Malajczuk & Theodorou, 1979) then these fluctuations represent transitions from conditions that allow Pc growth to conditions that promote host recovery.

There are two challenges in applying Laio's soil moisture model to the US southwest. The first is that rainfall along the US west coast is often more autocorrelated than assumed by Laio *et al.* (2001). The second is that interior and montane locations receive snow as well as rainfall, and that sustained snow melt provides an important contribution to local soil moisture dynamics.

We address the first of these challenges by noting that in a comprehensive sensitivity analysis of the Pc risk model used here, Pc risk was near-constant along contours of equivalent mean monthly rainfall (Thompson *et al.*, 2013). Pc risk is thus insensitive to the details of rainfall arrival at daily timescales, including deviations from a Poisson-process. This finding also allows us to directly use model data that forecasts monthly scale rainfall, without having to assume a model for the rainfall occurrence rates and depths. Throughout, therefore, we assume a rain-day frequency of $\lambda = 0.3$ (i.e., one rainy day in every 3 days), and estimate the average rainfall depth as $\alpha = \overline{P}/\lambda$ where $\overline{P}$ is the mean daily rainfall estimated from the monthly climate data.

In the absence of snow, the soil moisture probability density function (PDF) is estimated as a function of precipitation rate and depth (constrained to match the monthly precipitation totals), potential evaporation, soil depth, and soil properties, directly following the mathematical formulation in Laio *et al.* (2001). The presence of a snowpack invalidates this approach by generating a long transient condition which cannot be captured by the steady-state approximation used in deriving the PDF when soil moisture is controlled by rainfall. It is clear that if persistent snow-melt occurs then soils will be saturated, that is, $s = 1$ during the spring period when a snow-pack is in place. The simplest, and not far-from realistic approach is to assume that in any pixel containing a snow-pack with SWE >5 mm, $s = 1$, and that the probability of this saturated condition occurring throughout the spring period is equal to $P(s = 1) = \Sigma M_{SWE>5\ mm}/\Sigma M_{Spring}$, where $M_{SWE>5\ mm}$ indicates the number of months where a snowpack was present, and M_{Spring} indicates months in the Spring period. The remainder of the PDF is given by the precipitation-driven soil moisture conditions, weighted by $1 - P(s = 1)$. Effectively, this approximation represents the transient conditions of dry-down of the soil following melting of the snowpack, modified to account for the probability mass at $s = 1$. For the purposes of constraining the Pc dynamics, the dynamics of this transient condition are not critical, since the snowpack maintains soil in a wet condition that supports Pc growth during the period after snowmelt. Thus, this approximation is suitable for the purposes of Pc range determination.

Independently from the soil moisture PDF, the model incorporates a biological component that describes a simplified host–pathogen interaction. If we assume that the soil water potential exceeds Ψ_c, the pathogen colonizes the root zone of the host plant at a rate r_{max}. A healthy host has root volume v which is equal to its upper limit v_{max}. Infected roots eventually die, so that in an infected tree, the volume of colonized roots b lies between 0 (uninfected host) and v_{max} (root system completely colonized). Hosts with high resistance to Pc regrow roots rapidly or resist infection at a rate m (Newhook & Podger, 1972; Weste & Taylor, 1987), leading to a reduction in b. In dry soils, the rate of Pc growth is impeded to a 'drought' rate r_{min}, during which time the host will tend to recover. These dynamics can be expressed in a one-equation non-dimensional model (Thompson *et al.*, 2013), which reproduces the dynamics of a more complete two-equation susceptible-infected (SI) disease model. Here, $B = b/v_{max}$, $t' = tm$, $R_{max} = r_{max}/m$ and $R_{min} = r_{min}/m$, so that the final growth equation takes the form (Thompson *et al.*, 2013):

$$\begin{aligned} \frac{dB}{dt'} &= B(R(\Psi) - 1 - B^{\chi}), \\ R(\Psi) &= R_{max}, \quad \Psi > \Psi_c \\ &= R_{min}, \quad \Psi \leq \Psi_c \end{aligned} \tag{3}$$

The power χ in this equation is set to 100 for computational purposes: this provides a close approximation to a stepwise function in which pathogen colonization rates remain constant until the whole root zone is colonized, and then switches to zero. Provided $R_{min} < 1$ and $R_{max} > 1$, the steady state condition of this equation switches when soil is wet ($B = 1$, the whole root zone is colonized by Pc) and when soil is dry ($B = 0$, no pathogen remains in the system). This satisfies the

conditions for applying an analytical solution for the steady-state PDF of the pathogen extent B as derived by Horsthemke & Lefever (1984). As shown in Thompson *et al.* (2013), this steady state PDF has the form:

$$p(B_r) = -N'(R_{\max} - R_{\min})B^{a_1}(1 - R_{\max} + B^n)^{a_2}(1 - R_{\min} - B^n)^{a_3} \tag{4}$$

where

$$\begin{aligned} a_1 &= -\left(1 + \frac{f^+}{R_{\min} - 1} + \frac{f^-}{R_{\max} - 1}\right) \\ a_2 &= \frac{f^-}{n(R_{\max} - 1)} - 1 \\ a_3 &= \frac{f^+}{n(R_{\min} - 1)} - 1 \end{aligned} \tag{5}$$

for $B \in [0,1]$, where f^+ and f^- are the frequencies of switching around the s_c condition (and can be obtained directly from the PDF of s as shown in Porporato *et al.*, 2001), and N' is a normalization constant chosen such that $\int_0^\infty p(B)\mathrm{d}B = 1$. The expectation of B, $\overline{B}$ can also be computed analytically from the soil, climate and pathogen parameters, and provides a parsimonious metric of the risk posed by Pc for a given set of environmental and host conditions.

This model allows estimation of the probability of Pc infecting its hosts' root zone as a function of soil properties, rainfall statistics and vegetation type. The model was validated for two case studies in Western Australia and one agricultural case study in Oregon. Because the long history of Pc in Western Australia (over 100 years; Shearer *et al.*, 2004) has allowed the pathogen to spread extensively, and because it has received detailed attention there and in agricultural settings, the case studies provide a more comprehensive opportunity to validate the ecohydrological model than the comparison with Californian data made in this study. Therefore, we briefly report the findings from these three case studies: (i) all 27 locations with established Pc disease reported by the Centre for Phytophthora Science and Management (http://www.cpsm.murdoch.edu.au/), across the approximately 1000 km by 1000 km southwestern region of Western Australia coincide with regions where $\overline{B} \geq 0.5$, and 23 of 27 occur in regions where $\overline{B} \geq 0.8$, suggesting a rate of Type 2 (predicting no Pc when Pc was in fact present) errors in the range of 0–15%; (ii) examination of disease frequency on contrasting soil types in an intensively monitored Pc affected 5 ×5 km forest plot (Batini & Hopkins, 1972) lead to a model prediction that Pc would occur two times as frequently on clay soils than on sandy soil; observations showed that Pc actually occurred 1.9 times as frequently on clay soils than on sandy soils; and (iii) Finally, the model reproduced the near-linear increase in Pc disease severity from 20% to 60% root destruction on irrigated blueberries as the irrigation rate was increased from 0.5 to 1 to 1.5 times evaporative demand (Bryla & Linderman, 2007). Details of these validation exercises are reported in Thompson *et al.* (2013).

Application to the southwest USA

The southwestern USA contains a climatically, geologically, and biologically diverse set of landscapes (Torregrosa *et al.*, 2013). Climatically, the region encompasses cool, humid, oceanic climates near the coast, arid interior valleys and deserts with continental climates, and montane and nivial uplands in the Sierra Nevada mountain ranges. Precipitation tends to be highly seasonal with the majority falling during a 4-month period from December to March. The diversity of climatic types is reflected in the diversity of terrestrial vegetation, with important vegetation communities including coastal rainforests, dry chapparal, Mediterranean oak savannas, montane forests, and subalpine regions (Barbour *et al.*, 2007). Within the study area, the California Floristic Province is recognized as a biodiversity hotspot (Myers *et al.*, 2000), and the state is home to over 7600 plant species (Baldwin *et al.*, 2012). The San Francisco Bay Area, which is used as a higher resolution case study maintains much of the same complexity of climate, geology, and biology, due to strong ocean-inland gradients in temperature and annual precipitation (Gilliam, 2002), and the activity of various tectonic faults in the region (Sloan, 2005).

The diversity of climate and soil types in the study area can be directly parameterized within the stochastic soil moisture and pathogen models. Note that we have allowed spatial variations in evaporative demand to be driven by radiation, temperature, and humidity (via the Priestly–Taylor equation), and have not incorporated an explicit treatment of varying vegetation cover on $E_{\max}$. The rationale for this lies in the fact that surface conductance (the physical term describing the effect of leaf area on evapotranspiration) loses sensitivity to LAI for low humidity (characteristic of the region) and LAI > 2, suggesting that the first order controls on $E_{\max}$ variation lie in energy limitation rather than vegetation characteristics (Leuning *et al.*, 2008). The diversity of the vegetation also presents a challenge for parameterization of the pathogen dynamics in the model. It is clearly not feasible to parameterize specific host resistance terms for Pc for all 7600 vascular plant species in the study area; furthermore assessments of susceptibility of the native vegetation to Pc are strikingly incomplete, and remain insufficiently quantitative to allow a direct comparison to be made. The problem is similar to applying this model to Pc in Western Australia, where far more work on Pc susceptibility has been performed. In that comparably biodiverse landscape, 3084 of the 5710 native plant species were found to be susceptible or highly susceptible to Pc infection (Shearer *et al.*, 2004). This determination, however, required intensive surveys of native vegetation in representative habitats, as well as comparative inoculation greenhouse trials (Shearer *et al.*, 2004), and still provides only qualitative information about the relative vulnerability of host plants. No comparable investigations have as yet taken place in the US south west, although numerous common native species are known to be vulnerable to Pc, including manzanita species (Swiecki *et al.*, 2003), chapparal species (e.g., *Ceanothus* sp.), Monterey pine, sycamore, western sword fern, coast live oak (Farr & Rossman, 2013), bay laurel and madrone (Fichtner *et al.*, 2010). In the absence of detailed observations of host–pathogen interactions for the diversity of species in Western Australia, we explored climate limitations on range using a combination of: (i) laboratory estimates

of Pc growth rates in sterile media and (ii) host resistance parameters (m) taken from a moderately susceptible host (the eucalyptus species Jarrah, *Eucalyptus marginata*) and estimated to be 0.1 day^{-1} (Thompson *et al.*, 2013). We have repeated this approach for the US southwest with the following rationalizations: (i) moderately susceptible host dynamics ensure that climate effects are clear. For highly susceptible hosts, climatic drivers are relatively unimportant, since any serendipitous infection is likely to lead to mortality. For unsusceptible hosts, climate is equally unimportant. Thus to explore the impacts of climate change, moderately susceptible host assumptions are sensible; (ii) Evidence from infections of common tree species (oaks, laurels, madrone) suggests that the hosts are indeed moderately susceptible to Pc, with infections most common in wet areas (Garbelotto *et al.*, 2006; Fichtner *et al.*, 2010) and mortality commonly associated with concurrent pest or drought stress (Fichtner *et al.*, 2010); (iii) for the sake of identifying climate sensitivity specifically, holding host vulnerability constant across the study area provides a useful control, and in the absence of more detailed information, is the most parsimonious modeling approach. As a check on the impacts of this assumption, we have also evaluated the sensitivity of the model results to a doubling or halving of host resistance.

The biological parameters R_{max} and R_{min} were estimated from the assumed value of $m = 0.1$ and laboratory observations of r_{min} and r_{max}. Pc growth rates in sterile media at 25 °C were 0.46 day^{-1} under well-watered conditions (r_{max}), and 0.07 day^{-1} under dry conditions (r_{min}) (Malajczuk & Theodorou, 1979). Because the US southwest contains a large range in temperature due to strong marine effects near the coast, continentality inland, and large mountain ranges, we extended the definition of r_{min} and r_{max} to incorporate temperature dependence. Shearer *et al.* (1987) noted that growth rates of Pc varied linearly with temperature, and found that growth declined to zero at $T = 4.9$ °C. We therefore fit linear relationships between the values of r_{min} and r_{max} obtained by [45] at 25 °C and assumed values of 0 at $T = 4.9$ °C, obtaining:

$$r_{max} = -0.1122 + 0.023T, \quad (6)$$

$$r_{min} = -0.171 + 0.0035T, \quad (7)$$

where T is the ambient temperature experienced by Pc in °C and is assumed here to be equal to the average air temperature.

We force the modified Laio model (Section Pc - soil moisture model) with the data outlined in *Data Sources* section and Table 1 estimate the soil moisture PDF. The contribution of the climate factors to the development of a mean soil moisture map for the region is illustrated in Fig. 1. We then estimate the biological parameters using the different surface temperature conditions. Then, we estimate the PDF of the Pc colonization extent with Eqn (4). We interpret the mean colonization extent as being proportional to the risk posed by Pc to host vegetation during its most active period in spring. We compute this risk during 2–3 month periods in spring: March to May and April to June, recognizing that warmer temperatures for the later period might be offset by reduced water availability, and vice versa, and take the total risk as the maximum experienced at any pixel during these two periods.

Risk estimates

In addition to spatially distributed estimates of the mean Pc colonization extent ($Risk_{Rainfall}$) and survival probability ($Risk_{WinterSurvival}$), we also generate a surface, $Risk_{Soil}$ accounting for the effect of soil type on Pc risk. On the basis of literature thresholds for organic matter content in soils that suppress or do not suppress Pc, we set $Risk_{Soil} = 1$ in soils where organic matter content was less than 5%, and $Risk_{Soil} = 0$ for higher organic matter soil types (Broadbent & Baker, 1974; Nesbitt *et al.*, 1979; Weste & Marks, 1987). This surface thus allows us to account for the dramatic reduction of Pc risks on organic-rich soils. In practice, however, the extent of these soil types in the study area was limited: less than 1% of the terrestrial soils in the Bay Area were suppressive by

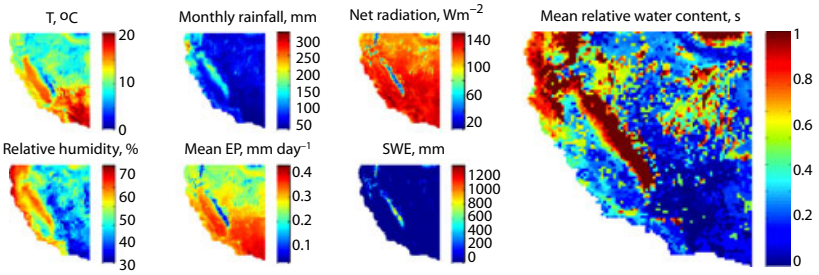

Fig. 1 Climatic factors that contribute to the soil moisture probability density functions (PDFs) across the state for the 1990–2000 climate conditions, averaged for the March to May period. Panels show the climatic components that contribute to the potential evaporation [temperature (T), relative humidity and net radiation], the resulting estimate of potential evaporation (mean EP) using the Priestly–Taylor equation, and the March snow-water equivalent (SWE). The panel on the right indicates the computed mean soil moisture (derived from full PDF estimates for each pixel) for the same period. There is a clear contribution of snowmelt that increases soil moisture toward saturation in the presence of snow cover. Desert features such as California's Central Valley and Arizona's deserts are clearly distinguished by the low soil moisture probabilities. Fine-scale variations in predicted soil moisture content also arise due to spatial differences in soil depth and clay content.

these metrics, and less than 2% of the soils in the whole study area. Thus, controls on Pc due to organic soils were limited.

To develop a metric of the total risk, we simply take the product of the three risk components:

$$\text{Risk}_{\text{Total}} = \text{Risk}_{\text{Rainfall}} \times \text{Risk}_{\text{Soil}} \times \text{Risk}_{\text{WinterSurvival}} \quad (8)$$

Areas where Risk $\longrightarrow 1$ have suitable thermal, moisture and soil organic matter conditions to support Pc. Areas where Risk $\longrightarrow 0$ are inhibited by spring being too dry, winter being too cold, the soil being too rich or a combination of these factors, and are thus at low risk of Pc infection. Based on our previous analysis of Pc distribution in Western Australia, where Pc risk was solely controlled by water availability (i.e., $\text{Risk}_{\text{soil}} = 1$ and $\text{Risk}_{\text{survival}} = 1$), Risk ≈ 0.5 delineates the limits of the Pc range. We then compare the projected risk maps for contemporary conditions in the southwest US and the Bay Area to the observed locations of Pc infection. Although these comparisons cannot identify false positives (regions where the model over-predicts the Pc risk), it does allow us to identify false negatives (i.e., regions where the model underestimates Pc risk).

Results

The model results are presented graphically in Figs 2 and 3 for the southwestern USA and for the Bay Area, respectively, for all climate scenarios. The spatial ranges over which there is an increase/decrease in Pc risk due to winter survival and spring Pc activity are also shown in Table 2. These results are discussed below in the light of the two guiding research questions.

How do climate and edaphic factors limit the potential range of Pc in the southwestern USA under contemporary conditions?

Winter survival. Predictions of winter survival of Pc are contingent on the performance of the soil temperature model. The error statistics for its application to the 16 CIMIS stations are shown in Table 3. The mean absolute error is 1.7 °C, and the mean total error is (−0.6 °). These errors lead to uncertainty in the projected winter-survival range of approximately ±3.5%, suggesting that the survival model predictions are robust to the error in the temperature model. This robustness reflects the fact that the survival probabilities depend on both threshold dynamics and cumulative temperatures. Absolute errors in temperature model predictions therefore tend to compensate for each other in the survival model. Winter survival predictions for the whole southwest area are shown in the top row of plots in Fig. 2 and are listed in Table 2. Under contemporary conditions, winter survival is plausible over an approximately 536 000 ± 18 000 km^2 area, or 43 ± 1.5% of the region. Applying the soil temperature model to the Bay Area indicates that 100% winter survival is likely under current conditions, which generate only occasional sub-zero temperatures.

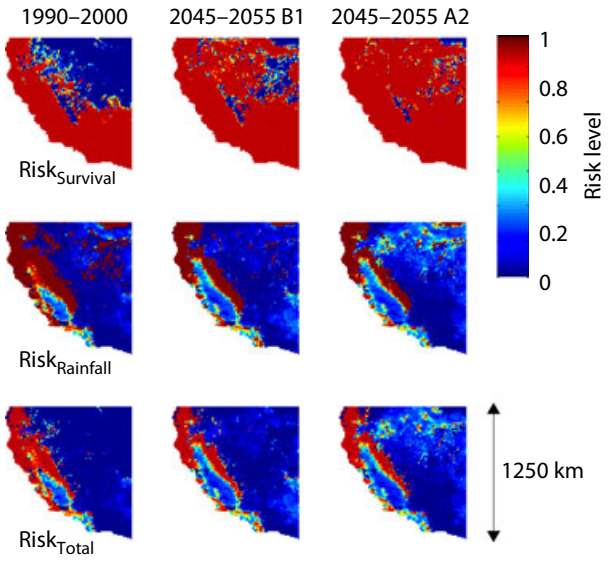

Fig. 2 The contributing, climate-driven and cumulative risk factors for *Phytophthora cinnamomi* (Pc) shown for the whole study area in California, Oregon, Nevada and Arizona. Columns of plots indicate the model predictions of risk under different climate scenarios. The rows of figures relate to the changing risk of Pc surviving over winter ($\text{Risk}_{\text{Survival}}$, top), or Pc receiving sufficiently warm and wet spring conditions to pose a risk to hosts with moderate susceptibility ($\text{Risk}_{\text{Rainfall}}$, middle) and the areas in which all of winter survival, spring conditions and non-suppressive soil conditions suggest Pc could potentially exist ($\text{Risk}_{\text{Total}}$, bottom). The legend is applicable to all plots, as the risk levels in each case are valued in the range 0–1.

Soil moisture and pathogen activity. The predicted Pc risk based on its spring activity is illustrated in the second row of plots in Fig. 2 and is listed in Table 2. The spatial pattern of elevated $\text{Risk}_{\text{rainfall}}$ reflects both the pattern of soil moisture availability and of spring temperatures (illustrated in Fig. 1). Approximately 327 000 km^2 of the study area (26%) is sufficiently warm and wet during the spring to support a high level of Pc activity.

In the San Francisco Bay Area, the pattern of $\text{Risk}_{\text{Total}}$ exhibits fine-scale spatial heterogeneity, which, given the low occurrence of organic soils and the 100% winter survival rate, may be attributed to fine-scale heterogeneity in $\text{Risk}_{\text{Rainfall}}$ (see Fig. 3). Much of this heterogeneity arises due to highly variable spatial soil properties. The major soil types follow a strongly anisotropic pattern in parent material that is aligned along the northwest–south-east direction of the major tectonic faults that occur in the region. Layered onto this heterogeneity is a markedly orographic rainfall pattern, with

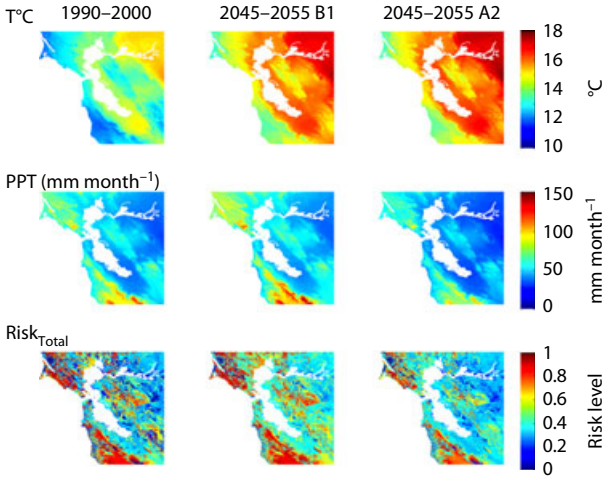

Fig. 3 Climate factors and projected *Phytophthora cinnamomi* (Pc) risk for the San Francisco Bay Area. The columns of plots indicate the different climate scenarios used in the modeling. The rows indicate the projected changes in mean spring temperature (T°C, top), mean monthly spring rainfall (PPT, middle) and the estimated Pc risk ($Risk_{Total}$, bottom). Note that because Pc survives winter in the Bay Area in all scenarios, and high carbon soils are not prevalent, $Risk_{Rainfall} \approx Risk_{Total}$ in this area.

the highest rainfall occurring on the marine side of the coastal ranges. Near the coast, Pc risk tends to increase with temperature, with the median risk increasing from 0.25 to 0.75 as temperature increases from 11 °C to 12.4 °C. Further inland, Pc risk plateaus and then declines with further temperature increases, reflecting the correlation between temperature and water stress once coastal influences wane.

Given the uncertainty associated with the estimated vegetation parameters, the soil moisture and pathogen activity modeling for the 1990–2000 period was repeated using the assumption that: (i) vegetation susceptibility was doubled ($m = 0.05$) and (ii) vegetation susceptibility was halved ($m = 0.2$). In case (i) we found that the overall spatial pattern of Pc risk was similar, but that in some regions where we projected no Pc risk for moderately susceptible vegetation, we would now project minor risks ($Risk_{Rainfall} \approx 0.25$) for the more sensitive vegetation. The overall range where $Risk_{Rainfall} > 0.5$ increased by 14%, or some 5% of the study region – comparable to the error associated with the soil temperature model. Comparable reductions in the range of Pc were found for case (ii) where the pattern of Pc risk was again maintained, but areas where we had projected low risk for moderately susceptible vegetation were not at risk for the resistant vegetation. The overall range where $Risk_{Rainfall} > 0.5$ decreased by 14%, or 5% of the study region, again comparable to the error due to the soil

Table 3 Error statistics compiled for running the soil temperature model for 16 CIMIS stations located across California. Stations include: Bishop, Calipatria/Mulberry, San Luis Obispo, Buntingville, Alturas, King City-Oasis Road, Victorville, Madera, Belridge, Otay Lake, Camarillo, Union City, Owens Lake South, Cadiz Valley, Woodland, Plymouth

Error metric	Mean error	Error standard deviation
Mean absolute error	1.68	0.66
Mean error	−0.66	1.31

Table 2 Spatial range of *Phytophthora cinnamomi* (Pc) in terms of projected total risk $Risk_{total}$, risk of winter survival $Risk_{survival}$, and risk during the spring season ($Risk_{rainfall}$) for the three climate scenarios at regional scales (an approximately 1000 by 1000 km area covering California and portions of neighboring states) and for the Bay Area (an approximately 150 by 150 km area covering the San Francisco Bay, stretching inland to Livermore, north to Napa and south almost to Santa Cruz). Figures given in parentheses indicate the percentage of the modeled domain represented by the given areas. To illustrate the complex interactions between temperature and water availability that govern the dynamic risk of Pc during spring growth, the area in which risk increases ($Risk_{Rainfall}\uparrow$) and decreases ($Risk_{Rainfall}\downarrow$) for each climate scenario is also shown

Scale	Scenario	$Risk_{Total} > 0.5$ $\times 10^5$ km^2	$Risk_{Survival} > 0.5$ $\times 10^5$ km^2	$Risk_{Rainfall} > 0.5$ $\times 10^5$ km^2	$Risk_{Rainfall}\uparrow$ $\times 10^5$ km^2	$Risk_{Rainfall}\downarrow$ $\times 10^5$ km^2
Regional	1990–2000	1.97 (15.6%)	5.36 (42.6%)	3.27 (25.9%)		
	2045–2055 B1	1.63 (13.0%)	8.21 (65.0%)	2.23 (17.7%)	3.90 (30.1%, 0.06↑)	4.01 (31.8%, 0.26↓)
	2045–2055 A2	1.74 (13.7%)	9.07 (71.8%)	2.20 (17.4%)	4.73 (37.3%, 0.08↑)	3.39 (26.7%, 0.28↓)
Scale	Scenario	Risk > 0.5 km^2	$Risk_{Survival} > 0.5$ km^2	$Risk_{Rainfall} > 0.5$	$Risk_{Rainfall}\uparrow$ km^2	$Risk_{Rainfall}\downarrow$ km^2
Bay Area	1970–2000	5384 (52.0%)	10 000 (100%)	5384 (52.0%)		
	2035–2065 B1	6514 (63.0%)	10 000 (100%)	6514 (63.0%)	817.4 (7.91%)	6 (0%)
	2035–2065 A2	3785 (36.6%)	10 000 (100%)	3785 (36.6%)	4.67 (0%)	1174 (11.4%)

temperature model. Thus, the relative change in Pc risk is: (i) significantly damped compared to relative change in host susceptibility and (ii) larger but comparable to other sources of error in the predictions.

Total contemporary Pc Risk. The contemporary area where $Risk_{Total}$ exceeds 0.5 covers 197 000 km^2 of the southwestern USA, or approximately 16% of the study region. Pc's potential range in the Bay Area covers approximately 52% of the terrestrial surface, some 5384 km^2. Note that the pixel in the regional model that corresponds to the Bay Area has $Risk_{Total} = 1$: the regional scale pixels do not account for spatial patterning *within* pixels. The total range of Pc is therefore likely to be overstated by the regional model due to small-scale, site-specific factors relating to orography, microclimate, and soil type.

Figure 4 presents a comparison of the estimated Pc risk under contemporary conditions with twelve locations in the state of California where Pc has been positively identified from soil baiting and diseased plants. Recently, Pc was also identified in a number of locations around the Bay Area, allowing a higher resolution comparison between observations and predicted risk to be made in this area. With one exception, all the observed occurrences of Pc are located in sites where the predicted risk levels were 0.8–1. The one site located in a region where we predicted negligible Pc risk is located within the Imperial Valley, an extensively irrigated agricultural region with an otherwise desert climatology. Thus, depending on how the Imperial Valley site is treated, the rate of Type 2 errors from the model was 0–8%. Although the number of sites where this comparison could be made was limited, the probability of randomly selecting 11 of 12 locations with $Risk_{Total} \geq 0.8$ is less than one in 10^7 across the whole model domain, and less than one in 10^4 for California specifically.

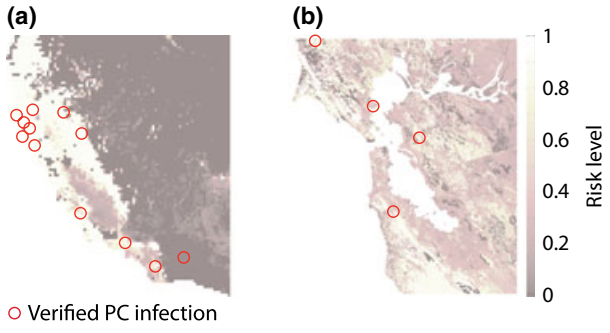

Fig. 4 Plot of observed *Phytophthora cinnamomi* (Pc) infection in CA (circles, red online, gray in print) overlaid on 1990–2000 (contemporary) risk projections at the scale of the southwest region and the scale of the San Francisco Bay Area. With the exception of a single site within the irrigated Imperial Valley, the observed Pc infection locations occur where the model indicates that $Risk_{Total} = 0.8–1.0$ (Jacobs *et al.*, 1997; Swiecki *et al.*, 2003, 2011; Garbelotto *et al.*, 2006; Rizzo & Fichtner, 2007; Elliott *et al.*, 2010; Fichtner *et al.*, 2010)

How do the different modes of Pc response to temperature and soil moisture change its projected range under plausible future climate scenarios?

The effects of a warming climate on Pc risk vary depending on the risk factors and specific climate scenario being assessed. Warming changes winter survival in a straightforward fashion: under the A2 scenario survival increases dramatically so that the region in which more than half of a Pc population would survive the winter increases from 43% (contemporary) to 72% of the study area. More modest increases in winter-survival probabilities arise under the B1 climate scenario, in which Pc winter survival becomes probable over 65% of the study area (Table 2).

The effects of climate change on soil moisture and Pc spring activity are more complex. At the regional scale, climate change reduces the risk posed by Pc (Fig. 2) across the majority of the study area. However, the changes are spatially variable. Pc risk declines markedly in the Central Valley. It is largely unchanged in coastal northern California and Oregon, where rainfall levels are projected to remain high. Its range is also unchanged in the south-eastern part of the region, which is significantly water limited under contemporary scenarios and projected to remain so. Pc risk increases in the north-eastern extent of the study area. The increase in Pc risk in this area is greatest in the high emissions scenario. In the lower emissions scenario, comparable increases in Pc extent occur inland in the southern extent of the range. In both cases, these increases indicate an interaction of warmer temperatures with unchanged or slightly enhanced rainfall.

The potential complexity of the interactions between changing water and temperature in one of these southern locations is illustrated in Fig. 5 for a site in the southwestern part of the region. In this location, Pc risk increases under the B1 scenario but decreases under the A2 scenario. Figure 5 shows a decomposition of the projected changes into those due to temperature and those due to changes in soil moisture. As shown, increasing temperatures increase Pc risk from the baseline case for both A2 and B1 scenarios, but in the A2 scenario, a decrease in soil moisture more than offsets the effect of warmer spring conditions. Conversely, under the B1 conditions, the slight increase in soil moisture increases pathogen risk at this location, but only when both temperature and soil moisture increase

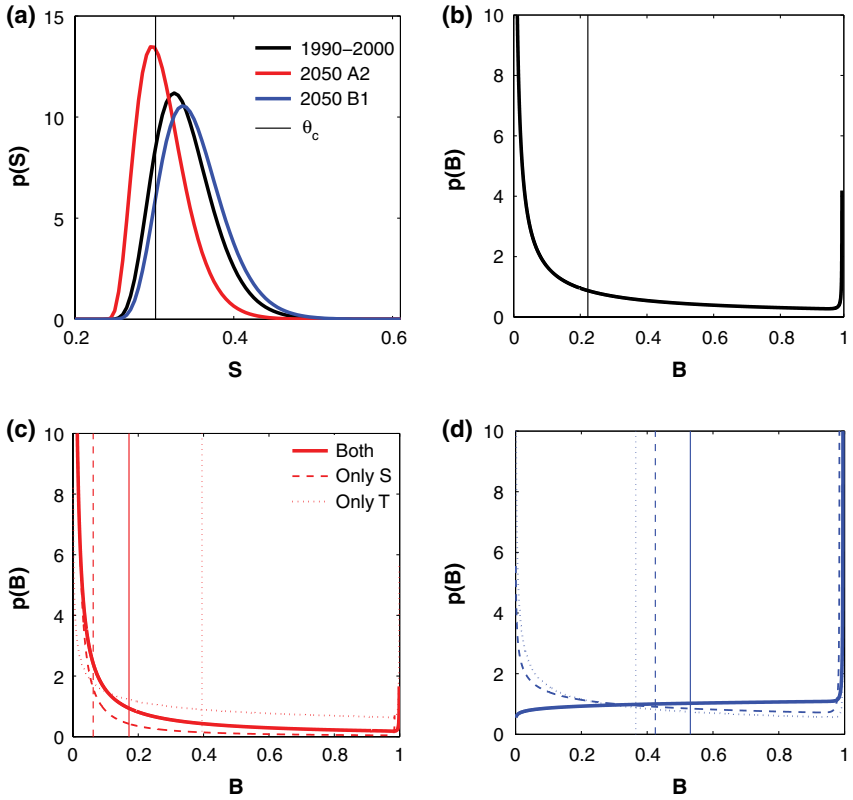

Fig. 5 Illustration of the complex interaction of temperature and water availability illustrated for an inland, montane location in California, located in the Sierra Nevada foothills inland from Santa Barbara. Here, temperature and rainfall both increase slightly for the B1 scenario, while temperature increases and rainfall decreases markedly for the A2 scenario. This leads to a slight decrease in relative soil moisture (*S*) for the A2 scenario and a slight increase for the B1 (a). Baseline $\text{Risk}_{\text{Rainfall}}$ (expressed as the root colonization extent, *B*) is shown in (b). (c) shows the projected PDF of *B* under the A2 scenario, and (d) shows the PDF of *B* under the B1 scenario, the vertical lines in (b–d) indicate the mean values of *B*. The B1 scenario generates a large increase in *Phytophthora cinnamomi* (Pc) risk, while the A2 scenario creates a decrease in risk. However, if the contributing factors are isolated [dashed and dotted lines in (c) and (d)], the increase in temperature in the A2 scenario causes an increase in Pc risk, which is more than offset by the decrease due to moisture limitation. In isolation, neither the temperature not precipitation increases in the B1 scenario would lead to any change in Pc risk, but their cumulative effect is to create a dramatic increase in overall risk.

together does the large predicted increase in pathogen risk occur. While these threshold-dynamics are not general across the study range, they illustrate the potential for highly nonlinear pathogen responses to interactions in changing temperature and moisture conditions, and highlight the importance of considering the impacts of synchronous changes in climate on pathogen dynamics.

As summarized in Table 2 and illustrated in Fig. 2, water limitation reduces Pc risk over a range of 340 000 km^2 across the region for the high emissions scenario, with an average decrease in the Pc risk of 0.28. Pc risk is reduced over 40 000 km^2 for the low emissions scenario, by 0.26 on average. Alleviation of thermal limitations on Pc growth rates increased the predicted Pc risk in an 470 000 km^2 area for the high emissions scenario with a projected mean increase of 0.08. For the low emissions scenario, Pc risks increase over a 390 000 km^2 area for the low emissions scenario, with an average 0.05 increase in the Pc risk. Overall, the total area where Pc risks exceed 0.5 declines to approximately 164 000 km^2 or 13% of the study region for the B1 scenario. The decline in spatial extent under a high emissions (A2) scenario is actually slightly *less* pronounced, with the predicted Pc range being 170 000 km^2 or 13.7% of the region. This occurs even though the area where there is sufficient water for high spring Pc activity declines more for the high emissions scenario than for a low emissions scenario. The results reflect the importance of a tradeoff between increased winter survival range and decreased spring water availability.

At the scale of the Bay Area, future climate projections contain considerable uncertainty associated with climatic downscaling. Broadly, however, the B1 scenario represents a case with warmer spring temperatures but without considerable reduction in rainfall,

while the A2 scenario represents a situation with reduced rainfall and warmer temperatures. As shown in Fig. 3, the effects are quite striking: an increase in temperature without a large decrease in rainfall results in an increase in the area that is vulnerable to Pc by approximately 20% (from approximately 5300–6500 km^2). Conversely, a decline in rainfall and increase in temperature result in a large decline in Pc risk, to approximately 3800 km^2, about half of its contemporary range.

Discussion

The modeling study indicated four different controls on modeled Pc range, which interacted to generate complex spatial patterns of Pc response to projected climatic changes. The first control was the proportion of soil organic carbon, which provided a static template of (isolated and restricted) areas in which Pc would not establish. The second control was winter temperatures which impede pathogen over-winter survival. The range over which the pathogen survived winter expanded sequentially from contemporary conditions to the B1 and then A2 climate scenarios. The third and fourth controls on pathogen range lay in spring temperature and rainfall which together controlled spring Pc activity. Declining precipitation in the B1 and A2 scenarios inhibited Pc growth. The implications of drier climatic conditions in the study area varied depending on the absolute local Pc risk in a given area. Thus, little change in Pc risk was predicted in wet regions such as the northern coast, where drier spring conditions under B1 and A2 climate futures were still wet enough to support Pc activity. In the driest limits of the current Pc range, contemporary rainfall was too limited to support Pc activity, and further drying of the climate under B1 and A2 scenarios did not alter the pathogen risk. In mesic regions, progressively dry springs reduced overall Pc risk under the B1 scenario, relative to contemporary conditions. Despite further reductions in rainfall under the A2 scenario, however, only minor further decreases in Pc spring risk were predicted compared to the B1 scenario. This we attribute to increasing spring temperatures enhancing the rate of Pc expansion during spring, which increased disease risk over part of the model range. The spatial locations where warmer spring temperatures under the B1 and A2 scenarios caused increases in Pc risk were spatially separated from the locations where decreases in rainfall reduced Pc risk, so the overall pattern of Pc risk during spring under contemporary, B1 and A2 scenarios differs: the B1 case primarily reflects reductions in the contemporary area of high risk, while the A2 scenario continues this reduction but also leads to expanded regions of moderate Pc risk in the north-eastern part of the study region. The interactions of these controls lead to a decrease in Pc range under both B1 and A2 scenarios compared to contemporary conditions, but, surprisingly, less of a reduction in total Pc range under the more extreme warming scenario.

The modeling study ignored several factors that impact dynamic Pc risk – that is, the risk of Pc developing in uninfected areas. It has not considered pathways of introduction of Pc into natural communities. Proximity to roads, streams, soil disturbance, innoculum sources, and high vehicle or pedestrian traffic are highly likely to impact these risks. Similarly, the diversity of Californian vegetation and its variable sensitivity to Pc has not been considered: higher resolution studies considering differentials of vegetation susceptibility could provide a far more nuanced picture of the spatial extent of Pc, and could, for instance, eliminate areas of risk in primarily urbanized environments in the San Francisco Bay Area. However, in the absence of improved data regarding host–pathogen interactions for dominant vegetation types in the area, there is limited basis on which to make such a high-resolution suite of assumptions about vegetation susceptibility. Despite this missing information, the damped sensitivity of Pc range relative to changes in assumed host resistance across the region in conjunction with field observations confirming that a wide range of regional species are susceptible to Pc, suggests that the overall conclusions of the modeling study regarding climate sensitivity should be robust. Finally, we have assumed that the local environmental conditions experienced by Pc are determined solely by climate, which is not true in the irrigated agricultural areas in California's Central and Imperial Valleys. In these regions, irrigation regimes that are sufficiently frequent to sustain high water potentials in the root zone would alleviate the environmental water stress, as indicated by the observation of Pc occurrence within the Imperial Valley. If water stress is alleviated in these regions, temperatures are warm enough in both winter and spring to support high levels of Pc activity. Thus, irrigated agricultural land should be considered at risk of Pc infestation under both present and future scenarios.

Overall, the modeling analysis suggests that Pc has a much larger potential range in the US southwest than could be inferred purely from current observations of the locations of infected sites. At present, despite the high awareness of *Phytophthora ramorum* and sudden oak death in the US southwest, there is limited public awareness, policy or scientific attention given to Pc (Swiecki *et al.*, 2011). Sources of Pc are known to exist in agricultural and nursery settings in California (including nurseries supplying native plants that are

used for revegetation, and could therefore export the disease into native ecosystems), and appear to be the source of Pc infection in native ecosystems in several cases (Zentmyer, 1980; Swiecki *et al*., 2011). However, no current phytosanitation certification programs, protocols for reducing soil movement from infected to clean sites, or recognized successful spot treatment approaches to minimizing Pc spread are in place in California (Dunstan *et al*., 2009; Swiecki *et al*., 2011). While the number of native species in California that are susceptible to Pc remains unclear, estimates in comparably biodiverse southwestern Australia suggest that over 3000 of the 5700 indigenous plant species are susceptible (Shearer *et al*., 2004). Pc has already demonstrated its potential to reshape plant communities and entire ecologies (Garkaklis *et al*., 2004). In the absence of detailed information about host susceptibility in California, the large ranges that appear to be supported by contemporary climates in conjunction with the severe effects of Pc in comparable ecosystems point to a critical need to improve risk assessment, phytosanitation and awareness of Pc disease.

Despite its relatively simple ecology, Pc nonetheless displays non-monotonic responses to climatic warming at regional and local scales, with spatially distinct regions having opposite trends in Pc risk. Although the modeling framework presented accounts for many different aspects of climate, other changes including carbon fertilization due to enhanced atmospheric [CO_2], changing land use and ecological thresholds have been neglected, and linking disease risk models to ecosystem outcomes remains challenging. For example, in Western Australia a 40 year drying trend has reduced Pc activity, but with the effect of replacing Pc induced mortality with drought stress stress (Brouwers *et al*., 2013). Considering that Pc mortality is linked to periods of drought stress that follow wet periods in which Pc causes root damage (Desprez-Loustau *et al*., 2006), limitation of Pc range due to drying, while beneficial for limiting expansion of the pathogen, may come at the expense of increased mortality for infected ecosystems.

Acknowledgements

Support from the National Science Foundation (NSF EAR-1013339) is acknowledged.

References

Agrios G (2005) *Plant Pathology*. Elsevier Academic Press, San Diego, CA.

Allen CD, Macalady AK, Chenchouni H *et al*. (2010) A global overview of drought and heat-induced tree mortality reveals emerging climate change risks for forests. *Forest Ecology and Management*, **259**, 660–684.

Balci Y, Halmschlager E (2003) Incidence of *Phytophthora* species in oak forests in Austria and their possible involvement in oak decline. *Forest Pathology*, **33**, 157–174.

Baldwin B, Goldman D, Keil D, Patterson R, Rosatti T, Wilken D (2012) *The Jepson Manual: Vascular Plants of California* (2nd edn). University of California Press, Berkeley, CA.

Barbour M, Keeler-Wolf T, Shoenheer AA (2007) *Terrestrial Vegetation of California*. University of California Press, Berkeley, CA.

Batini F, Hopkins E (1972) *Phytophthora cinnamomi* rands – a root pathogen of the Jarrah forest. *Australian Forestry*, **36**, 57–68.

Benjamin M, Newhook F (1981) Effect of glass microbeads on *Phytophthora* zoospore motility. *Transactions of the British Mycological Society*, **78**, 43–46.

Benson D, Grand L, Veria C, Gottwald T (2006) Temporal and spatial epidemiology of *Phytophthora* root rot in Fraser Fir plantations. *Plant Disease*, **90**, 1171–1180.

Bergot M, Cloppet E, Perarnaud V, Deque M, Marcais B, Desprez-Loustau ML (2004) Simulation of potential range expansion of oak disease caused by *Phytophthora cinnamomi* under climate change. *Global Change Biology*, **10**, 1539–1552.

Boland G, Melzer M, Hopkin A, Higgins V, Nassuth A (2004) Climate change and plant diseases in Ontario. *Canadian Journal of Plant Pathology*, **26**, 335–350.

Brasier CM, Scott JK (1994) European oak declines and global warming: a theoretical assessment with special reference to the activity of *Phytophthora cinnamomi*. *EPPO Bulletin*, **24**, 221–232.

Broadbent P, Baker K (1974) Behaviour of *Phytophthora cinnamomi* in soils suppressive and conducive to root rot. *Crop and Pasture Science*, **25**, 121–137.

Brouwers N, Matusick G, Ruthrof K, Lyons T, Hardy G (2013) Landscape-scale assessment of tree crown dieback following extreme drought and heat in a Mediterranean eucalypt forest ecosystem. *Landscape Ecology*, **28**, 69–80.

Bryla D, Linderman R (2007) Implications of irrigation method and amount of water application on *Phytophthora* and *Pythium* infection and severity of root rot in highbush blueberry. *HortScience*, **42**, 1463–1467.

Cayan D, Tyree M, Dettinger M *et al*. (2009) Climate change scenarios and sea level rise estimates for California – 2008 climate change scenarios assessment – final report. Available at: http://www.energy.ca.gov/publications/displayOneReport.php?pubNum=CEC-5 00-2009-014-F (accessed 20 June 2013).

Chakraborty S (2005) Potential impact of climate change on plant-pathogen interactions. *Australasian Plant Pathology*, **34**, 443–448.

Chakraborty S, Tiedemann AV, Teng PS (2000) Climate change: potential impact on plant diseases. *Environmental Pollution*, **108**, 317–326.

Chavarriaga D, Bodles WJA, Leifert C, Belbahri L, Woodward S (2007) *Phytophthora cinnamomi* and other fine root pathogens in north temperate pine forests. *FEMS Microbiology Letters*, **276**, 67–74.

Clapp R, Hornberger G (1978) Empirical equations for some soil hydraulic properties. *Water Resources Research*, **14**, 601–604.

Coakley S, Scherm H, Chakraborty S (1999) Climate change and plant disease management. *Annual Review of Phytopathology*, **37**, 399–426.

Collins WD, Bitz CM, Blackmon ML *et al*. (2006) The community climate system model version 3 (ccsm3). *Journal of Climate*, **19**, 2122–2143.

Desprez-Loustau ML, Marcais B, Nageleisen LM, Piou D, Vannini A (2006) Interactive effects of drought and pathogens in forest trees. *Annals of Forest Science*, **63**, 597–612.

Dunstan WA, Rudman T, Shearer BL *et al*. (2009) Containment and spot eradication of a highly destructive, invasive plant pathogen (phytophthora cinnamomi) in natural ecosystems. *Biological Invasions*, **12**, 913–925.

Elliott M, Chastagner G, Dermott G, DeBauw A, Sniezko R (2010) A first look at genetic variation in resistance to the root pathogen *Phytophthora cinnamomi* using a range-wide collection of pacific madrone *Arbutus menziesii*. In: *Proceedings of the 4th International Workshop on Genetics of Host-Parasite Interactions in Forestry*, General Technical Report PSW-GTR-240, pp. 290–294. US Forest Service, Albany, CA. Available at: http://www.fs.fed.us/psw/publications/documents/psw_gtr240/ps w_gtr240_290.pdf (accessed 17 December 2013).

Fabre B, Piou D, Desprez-Loustau ML, Marcais B (2011) Can the emergence of pine Diplodia shoot blight in France be explained by changes in pathogen pressure linked to climate change? *Global Change Biology*, **17**, 3218–3227.

Farr D, Rossman A (2013) Fungal database. Available at: http://nt.ars-grin.gov/fungaldatabases/ (accessed 12 September 2013).

Fichtner EJ, Rizzo DM, Swiecki TJ, Bernhardt EA (2010) Emergence of *Phytophthora cinnamomi* in a Sudden Oak Death-impacted forest. In: *Proceedings of the Sudden Oak Death Fourth Science Symposium*, General Technical Report PSW-GTR-229, pp. 320–321. US Forest Service, Santa Cruz, CA.

Flint L, Flint A (2012) Downscaling future climate scenarios to fine scales for hydrologic and ecological modeling and analysis. *Ecological Processes*, **1**, 1–15.

Garbelotto M, Huberli D, Shaw D (2006) First report on an infestation of *Phytophthora cinnamomi* in natural oak woodlands of California and its differential impact on two native oak species. *Plant Disease*, **90**, 685.

Garkaklis MJ, Calver MC, A WB, Hardy GES (2004) Habitat alteration caused by introduced plant disease: a significant threat to the conservation of Australian forest fauna. In: *Conservation of Australians Forest Fauna* (ed. Lunney D), pp. 899–913. Royal Zoological Society of New South Wales, Mosman, NSW.

Garrett KA, Dendy SP, Frank EE, Rouse MN, Travers SE (2006) Climate change effects on plant disease: genomes to ecosystems. *Annual Review of Phytopathology*, **44**, 489–509.

Gilliam H (2002) *Weather of the San Francisco Bay Region* (2nd edn). University of California Press, Berkeley, CA.

Harham A (2005) *Phytophthora cinnamomi*. *Molecular Plant Pathology*, **6**, 589–604.

Horsthemke W, Lefever R (1984) *Noise-induced Transitions: Theory and Applications in Physics, Chemistry and Biology*. Springer, New York.

Hwang SC, Ko W (1978) Biology of chlamydospores, sporangia, and zoospores of *Phytophthora cinnamomi* in soil. *Phytopathology*, **68**, 726–731.

Ibanez I, Clark J, Dietze M *et al*. (2006) Predicting biodiversity change: outside the climate envelope, beyond the species-area curve. *Ecology*, **87**, 1896–1906.

Jacobs K, MacDonald JD, Berry AM, Costello LR (1997) The effect of low oxygen stress on *Phytophthora cinnamomi* infection and disease of cork oak roots. In: *Proceedings of the Symposium on Oak Woodlands: Ecology, Management, and Urban Interface Issues*, USDA Forest Service General Technical Report PSW-GTR-160, pp. 553–558. US Forest Service, San Luis Obispo, CA. Available at: http://www.fs.fed.us/psw/publications/documents/psw_gtr160/ps w_gtr160_04g_jacobs.pdf (accessed 17 December 2013).

Jactel H, Petit J, Desprez-Loustau ML, Delzon S, Piou D, Battisti A, Koricheva J (2012) Drought effects on damage by forest insects and pathogens: a meta-analysis. *Global Change Biology*, **18**, 267–276.

Jönsson U (2006) A conceptual model for the development of *Phytophthora* disease in *Quercus robur*. *New Phytologist*, **171**, 55–68.

Judelson H, Blanco F (2005) The spores of *Phytophthora*: weapons of the plant destroyer. *Nature Reviews Microbiology*, **3**, 47–58.

Kang S, Kim S, Oh S, Lee D (2000) Predicting spatial and temporal patterns of soil temperature based on topography, surface cover and air temperature. *Forest Ecology and Management*, **136**, 173–184.

Kätterer T, Andrön O (2008) Predicting daily soil temperature profiles in arable soils in cold temperate regions from air temperature and leaf area index. *Acta Agriculturae Scandinavica, Section B – Soil & Plant Science*, **59**, 77–86.

Laio F, Porporato A, Ridolfi L, Rodriguez-Iturbe I (2001) Plants in water-controlled ecosystems: active role in hydrologic processes and response to water stress – II. Probabilistic soil moisture dynamics. *Advances in Water Resources*, **24**, 707–723.

Lake JA, Wade RN (2009) Plant-pathogen interactions and elevated CO_2: morphological changes in favor of pathogens. *Journal of Experimental Botany*, **60**, 3123–3131.

Leuning R, Zhang YQ, Rajaud A, Cleugh H, Tu K (2008) A simple surface conductance model to estimate regional evaporation using MODIS leaf area index and the Penman-Monteith equation. *Water Resources Research*, **44**, doi: 10.1029/2007WR006562.

MacDonald J, Duniway J (1978) Influence of the matric and osmotic components of water potential on zoospore discharge in of *Phytophthora*. *Ecology and Epidemiology*, **67**, 751–757.

Malajczuk N, Theodorou C (1979) Influence of water potential on growth and cultural characteristics of *Phytophthora cinnamomi*. *Transactions of the British Mycological Society*, **72**, 15–18.

Marçais B, Dupuis F, Desprez-Loustau M (1996) Modelling the influence of winter frosts on the development of the stem canker of red oak, caused by *Phytophthora cinnamomi*. *Annales des Sciences Forestières*, **53**, 369–382.

Maurer E, Wood A, Adam J, Lettenmaier D, Nijssen B (2002) A long-term hydrologically-based data set of land surface fluxes and states for the conterminous United States. *Journal of Climate*, **15**, 3237–3251.

Melloy P, Hollaway G, Luck J, Norton R, Aitken E, Chakraborty S (2010) Production and fitness of *Fusarium pseudograminearum* inoculum at elevated carbon dioxide in FACE. *Global Change Biology*, **16**, 3363–3373.

Myers N, Mittermeier RA, Mittermeier CG, da Fonseca GAB, Kent J (2000) Biodiversity hotspots for conservation priorities. *Nature*, **403**, 853–858.

Nesbitt H, Malajczuk N, Glenn A (1978) Effect of soil moisture and temperature on the survival of *Phytophthora cinnamomi* rands in soil. *Soil Biology and Biochemistry*, **11**, 137–140.

Nesbitt HJ, Malajczuk N, Glenn AR (1979) Effect of organic matter on the survival of *Phytophthora cinnamomi* rands in soil. *Soil Biology and Biochemistry*, **11**, 133–136.

Newhook F, Podger F (1972) The role of *Phytophthora cinnamomi* in Australian and New Zealand forests. *Annual Reviews in Phytopathology*, **10**, 299–326.

Pagliaccia D, McKee B, Pond E, Douhan GW (2011) Population genetic structure of *Phytophthora cinnamomi* associated with Phytophthora root rot of avocado (*Persea americana*) within California. *Phytopathology*, **101**, S135.

Pagliaccia D, Pond E, McKee B, Douhan GW (2013) Population genetic structure of *Phytophthora cinnamomi* associated with avocado in California and the discovery of a potentially recent introduction of a new clonal lineage. *Phytopathology*, **103**, 91–97.

Pangga IB, Chakraborty S, Yates D (2004) Canopy size and induced resistance in *Stylosanthes scabra* determine anthracnose severity at high CO_2. *Phytopathology*, **94**, 221–227.

Pangga IB, Hanan J, Chakraborty S (2011) Pathogen dynamics in a crop canopy and their evolution under changing climate. *Plant Pathology*, **60**, 70–81.

Pautasso M, Dehnen-Schmutz K, Holdenrieder O *et al*. (2010) Plant health and global change – some implications for landscape management. *Biological Reviews*, **85**, 729–755.

Pautasso M, Doering TF, Garbelotto M, Pellis L, Jeger MJ (2012) Impacts of climate change on plant diseases-opinions and trends. *European Journal of Plant Pathology*, **133**, 295–313.

Peters-Lidard CD, Blackburn E, Liang X, Wood EF (1998) The effect of soil thermal conductivity parameterization on surface energy fluxes and temperatures. *Journal of the Atmospheric Sciences*, **55**, 1209–1224.

Porporato A, Laio F, Ridolfi L, Rodriguez-Iturbe I (2001) Plants in water-controlled ecosystems: active role in hydrologic processes and response to water stress – III. Vegetation water stress. *Advances in Water Resources*, **24**, 725–744.

Rizzo D, Fichtner E (2007) Phytophthora in forests and natural ecosystems of the Americas. In: *Proceedings of the Fourth Meeting of the International Union of Forest Research Organizations (IUFRO) Working Party S07.02.09*, General Technical Report PSW-GTR-221, pp. 35–44. US Forest Service, Monterey, CA. Available at: http://ucanr.edu/sites/rizzolab/files/142694.pdf#page=47 (accessed 17 December 2013).

Scharwz G, Alexander RB (1995) Soils data for the conterminous United States derived from the NRCS State Soil Geographic (STATSGO) Database. Available at: http://water.usgs.gov/lookup/getspatial?ussoils (accessed 17 December 2013).

Shea S, Shearer B, Tippett J, Deegan P (1983) Distribution, reproduction and movement of *Phytophthora cinnamomi* on sites highly conducive to Jarrah Dieback in South Western Australia. *Plant Disease*, **67**, 970–973.

Shearer B, Shea S, Deegan P (1987) Temperature-growth relationships of *Phytophthora cinnamomi* in the secondary phloem of roots of *Banksia grandis* and *Eucalyptus marginata*. *Phytopathology*, **77**, 661–665.

Shearer BL, Crane CE, Cochrane A (2004) Quantification of the susceptibility of the native flora of the south-west botanical province, Western Australia, to *Phytophthora cinnamomi*. *Australian Journal of Botany*, **52**, 435–443.

Sloan D (2005) *Geology of the San Francisco Bay Region*. University of California Press, Berkeley, CA.

Staff SS (2012) Soil Survey Geographic (SSURGO) database for California. Available at: http://websoilsurvey.sc.egov.usda.gov/App/HomePage.htm (accessed 17 December 2013).

Sutherst RW, Constable F, Finlay KJ, Harrington R, Luck J, Zalucki MP (2011) Adapting to crop pest and pathogen risks under a changing climate. *Wiley Interdisciplinary Reviews-Climate Change*, **2**, 220–237.

Swiecki TJ, Bernhardt EA, Garbelotto M (2003) First report of root and crown rot caused by *Phytophthora cinnamomi* affecting native stands of *Arctostaphylos myrtifolia* and *A. viscida* in California. *Plant Disease*, **87**, 1395.

Swiecki TJ, Bernhardt E, Garbelotto M, Fichtner E (2011) The exotic plant pathogen *Phytophthora cinnamomi:* a major threat to rare *Acrtostaphylos* and much more. *Proceedings of the CNPS Conservation Conference* (eds. Willoughby JW, Orr BK, Schierenbeck KA, Jensen NJ), 17–19 January 2009, Sacramento, CA, 367–371.

Thompson S, Alvarez-Loayza P, Terborgh J, Katul G (2010) The effects of plant pathogens on tree recruitment in the Western Amazon under a projected future climate: a dynamical systems analysis. *Journal of Ecology*, **98**, 1434–1446.

Thompson S, Levin S, Rodriguez-Iturbe R (2013) Linking plant disease risk and precipitation drivers: a dynamical systems framework. *The American Naturalist*, **181**, E1–E16.

Tidwell TE, Kosta KL, Henderson JC (1984) Root rot of Western Swordfern *Polystichum munitum* caused by *Phytophthora cinnamomi* in California USA. *Plant Disease*, **68**, 536.

Tippett J, Crombie D, Hill T (1987) Effect of phloem water relations on the growth of *Phytophthora cinnamomi* in *Eucalyptus marginata*. *Phytopathology*, **77**, 246–250.

Tippett J, McGrath J, Hill T (1989) Site and seasonal effects on susceptibility of *Eucalyptus marginata* to *Phytophthora cinnamomi*. *Australian Journal of Botany*, **37**, 481–490.

Torregrosa A, Taylor MD, Flint LE, Flint AL (2013) Present, future, and novel bioclimates of the San Francisco, California region. *PLoS ONE*, **8**, e58450.

van Vuuren D, Edmonds J, Kainuma M *et al*. (2011) The representative concentration pathways: an overview. *Climatic Change*, **109**, 5–31.

Weste G, Law C (1973) The invasion of native forest by *Phytophthora cinnamomi*. III. Threat to the National Park, Wilson's Promontory, Victoria. *Australian Journal of Botany*, **21**, 31–51.

Weste G, Marks GC (1987) The biology of *Phytophthora cinnamomi* in Australasian forests. *Annual Review of Phytopathology*, **25**, 207–229.

Weste G, Taylor P (1987) The invasion of native forest by *Phytophthora cinnamomi*. I. Brisbane Ranges, Victoria. *Australian Journal of Botany*, **19**, 281–294.

Zentmyer GA (1980) *Phytophthora cinnamomi and the Diseases it Causes*. *10*. American Phytopathological Society, St. Paul, MN.

Zentmyer G, Leary J, Klure LJ, Grantham G (1976) Variability in growth of *Phytophthora cinnomomi* in relation to temperature. *Phytopathology*, **66**, 982–986.

Zheng D, Hunt ER Jr, Running SW (1993) A daily soil temperature model based on air temperature and precipitation for continental applications. *Climate Research*, **2**, 183–191.

Supporting Information

Additional Supporting Information may be found in the online version of this article:

Appendix S1. Soil thermal diffusivity estimates.